

Finite Element Analysis of Tibia with Osteogenesis Imperfecta: The Influence of Considering Cancellous Bone in Model Reconstruction

H.Y. Tan¹, K.S. Basaruddin^{1*}, M.H. Mat Som¹, S.F. Khan¹, A.R. Sulaiman² and A. Shukrimi³

¹Biomechanics and Biomaterials Research Group, School of Mechatronic Engineering, Universiti Malaysia Perlis, Pauh Putra Campus, 02600, Arau, Perlis.

²Department of Orthopaedics, School of Medical Science, Universiti Sains Malaysia, 16150 Kubang Kerian, Kelantan, Malaysia.

³Department of Orthopaedics, Kulliyyah of Medicine, International Islamic University Malaysia, 25710 Kuantan, Pahang, Malaysia

*Corresponding author: khsalleh@unimap.edu.my

Abstract-- The paper aims to develop the finite element (FE) models of tibia with Osteogenesis Imperfecta (OI) based on a patient-specific computed tomography (CT)-images. Two types of FE model have been developed. The first model was set the tibia bone as a single solid model whereas the second model consists of cortical bone and cancellous bone. The developed FE models were used for FE analysis using Voxelcon under various loadings, and then the results of the different models were compared. It was found that the single model yields relatively in agreement to piecewise model, with percentage different of below than 2% for all loading conditions. It seems that the reconstructed FE model considering the cancellous bone did not give significant effect compared to the solid model that neglecting the microstructure of cancellous bone. Hence, we can conclude that the single solid FE model with OI has predicted well, at least for the present boundary conditions, although the cancellous bone was neglected in the model reconstruction.

1. INTRODUCTION

Osteogenesis Imperfecta (OI), also known as brittle bone disease, is a genetic bone fragility disorder characterized by bone deformities. OI is among the most commonly found bone fragility disorder in children, and has a statistical incidence of 1 in 10,000 to 1 in 20,000 newborns. OI is a heterogeneous disorder and can be categorized into four main types based on clinical, radiographic, and genetic criteria, namely type I, type II, type III, and type IV [1]. Among these four types of OI, OI type II is known as one of the most lethal form of OI and is regarded as one of the most regularly seen severe skeletal dysplasia [2].

The study on human bone's stress-strain response through FE analysis has been carried out by many previous researchers [3]–[6]. One of the most common approach used was to obtain the image of human bone through CT scanning as performed by Garijo et al [3], where the authors constructed subject-specific FE model of tibia bone based on the CT image with specifications as followed: pixel size

0.977 mm, pixel resolution = 512 x 512 pixels, slice thickness = 3.00 mm, field of view (FOV) = 500.0 cm, and excitation voltage = 120 kV. The authors generated FE meshes by using 3-matic using linear tetrahedral elements with an element size of 3 mm. The authors eventually concluded that the CT image derived FE model has great potential for the estimation of stress-strain responses in human bones.

Gibbs et. al [4] also developed tibia FE model based on a variation of CT scanning technique called high-resolution peripheral quantitative computed tomography (HRpQCT) scan using a voxel conversion method. Consequently, the authors managed to carry out FE estimations of bone structure properties in terms of failure load, ultimate stress, stiffness, and cortical-to-trabecular load ratio. Tibia FE models were also developed for orthopedic purposes as demonstrated by González-Carbonell et. al [7], where the authors developed the FE models based on DICOM format images obtained from Computed Tomography Scanner GE Light-Speed VCT with the following specifications: pixel size = 0.773 mm, pixel resolution = 512 x 512 pixels, slice thickness = 5 mm, and excitation voltage = 120 kV. González-Carbonell et. al used Mimics for the reconstruction of the tibia bone model by using image segmentation method, and the FE models were used in FE software Abaqus and Hypermesh for FE analysis.

Besides reconstruction of tibia bone model based on CT images, there are also methods to develop FE models based on both CT and MRI images as performed by Koh et. al [8]. The authors' study involved soft tissues, therefore CT imaging and MRI imaging were used for development of bony and soft tissues respectively with slice thicknesses of 0.1 mm for CT scan and 0.4 mm for MRI scan. In order to combine both reconstructed models from different imaging technique, the authors defined the anatomic reference points of both of the models and then used positional alignment

technique to combine the two models in Rapidform software. The resultant solid model was imported into Hypermesh to generate FE model and then FE analysis was performed using Abaqus to investigate the contact stresses on the FE model.

In effort to investigate the effect of various loading on bones, some researchers developed patient-specific finite element (FE) models in order to carry out FE analysis [9]–[12]. These FE models are useful for the estimation of mechanical behaviours of subjects with various geometries, and can be constructed based on computed tomography (CT) or magnetic resonance imaging (MRI) images [13]. In the development of such FE models, researchers assigned respective material properties to cortical and cancellous bones. For instance, Weng et. al developed the FE model by assigning different material properties to the specific corresponding component such as cancellous and cortical bone [14]. Since cancellous bone is only found partially on the tibia bone structure, at the both of the distal end of the bone, hence this paper aims to investigate the influence of considering the cancellous bone in OI-affected bone model reconstruction for static stress analysis. If the results for both models (FE model considering cancellous bone and FE

model as a solid bone) are in agreement, FE model as a solid bone can be considered as a good enough for further analysis without considering cancellous bone that requires high number of element and computational cost.

2. MATERIALS AND METHODS

2.1 CT images of OI patient

A CT scanned images of tibia bone from an enrolled OI patient (13 years old, female) was provided by Hospital Universiti Sains Malaysia (HUSM). The images provided were in DICOM format with a size of 512 x 512 with 388 slices, each slice was allocated 16 bits storage and is stored as 12-bit images. There are two kind of images that were segmented, one of the segmented image had the tibia presented as a solid bone, while the other segmented image was split into image of cancellous bone and cortical bone. Those set of images were then processed using commercial software, Voxelcon (Quint Corp, Tokyo) for finite element modelling. The geometrical model of OI-affected bone that was reconstructed from the segmented images is shown in Figure 1.

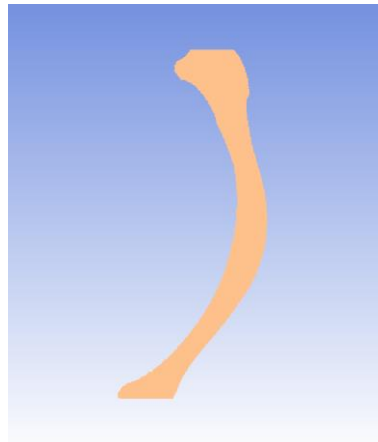


Fig. 1. Geometrical model of OI-affected bone

2.2 Reconstruction of tibia bone model for FEA

Finite element models for both set of segmented images were reconstructed in Voxelcon as a solid model using conversion of 1 mm³ voxel element for 1 volume pixel

image. The reconstructed model that was converted the image to a solid bone is shown in Figure 2, whereas Figure 3 shows the reconstructed FE model that consists of cortical and cancellous bone parts.

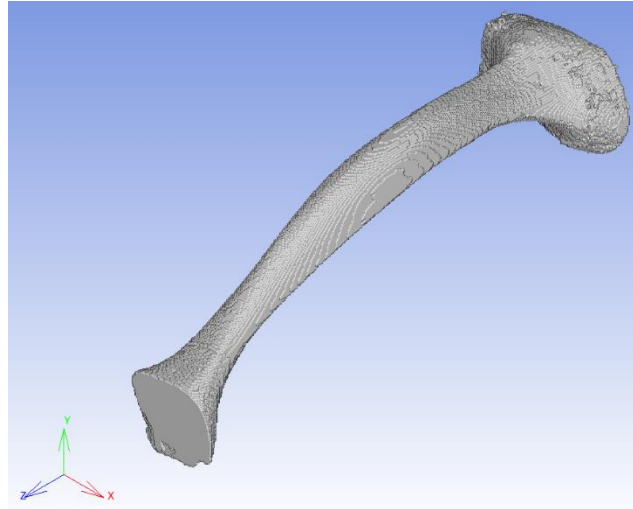
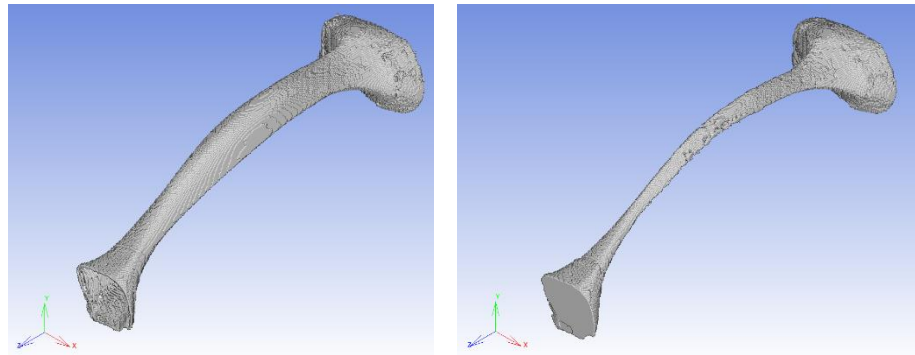


Fig. 2. Reconstructed FE model of a solid tibia with OI.



(a) cortical bone model

(b) cancellous bone model

Fig. 3. Reconstructed FE model that consist of cortical and cancellous bone.

2.3 Mechanical properties and boundary conditions

Both of the bone models were assumed to be isotropic and linearly elastic [15]. For the bone model with both cancellous and cortical part, the Young's modulus and Poisson's ratio values for cortical bone are 17 GPa and 0.33 respectively, while for cancellous bone the Young's modulus and Poisson's ratio values are 5 GPa and 0.33 respectively [14]. On the other hand, the Young's modulus and Poisson's ratio for the single unit bone model are 19 GPa and 0.3 respectively [16].

2.4 Boundary conditions and mechanical loading

For boundary condition, as shown in Figure 4, fixed boundary was applied at the end of the tibia model close to

ankle joint, while loads were applied at the end close to tibiofemoral joint. The mechanical loadings applied onto the tibia are divided into two categories, one of them are artificial loads imposed onto the bone model to test the stress-strain reactions on sagittal and coronal plane. On the other hand, the other set of loading consisted of loadings from activities of daily living (ADL) which includes loading from standing, walking, and running. For ADL, the loading force on tibiofemoral joint during standing is 1.07BW [17], while the loading force on tibiofemoral joint during walking and running are 2.83BW and 7.83BW [18] respectively. The loadings were applied for both models to investigate their stress-strain responses. For loading on sagittal coronal plane, the artificial loads imposed were 432N and 357.4N respectively.

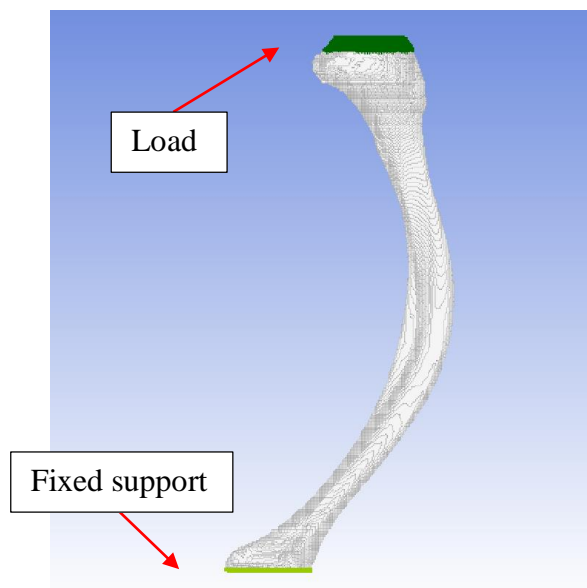


Fig. 4. Boundary conditions of tibia model

4. RESULTS AND DISCUSSION

Both tibia models were tested for von-Mises stress response where the results are presented in Figure 5. For ADL loads during standing, the single solid and cortical-cancellous models were subjected to von Mises stress of 1.39 MPa and 1.42 MPa respectively. During walking, the von-Mises stress

for single solid and cortical-cancellous models were 3.68MPa and 3.74MPa respectively, while during running the von-Mises stress for single solid and cortical-cancellous models were 10.17 MPa and 10.36 MPa respectively. All of the data pairs yielded a percentage difference of 1.82% between the single solid and cortical-cancellous 3D tibia FE models.

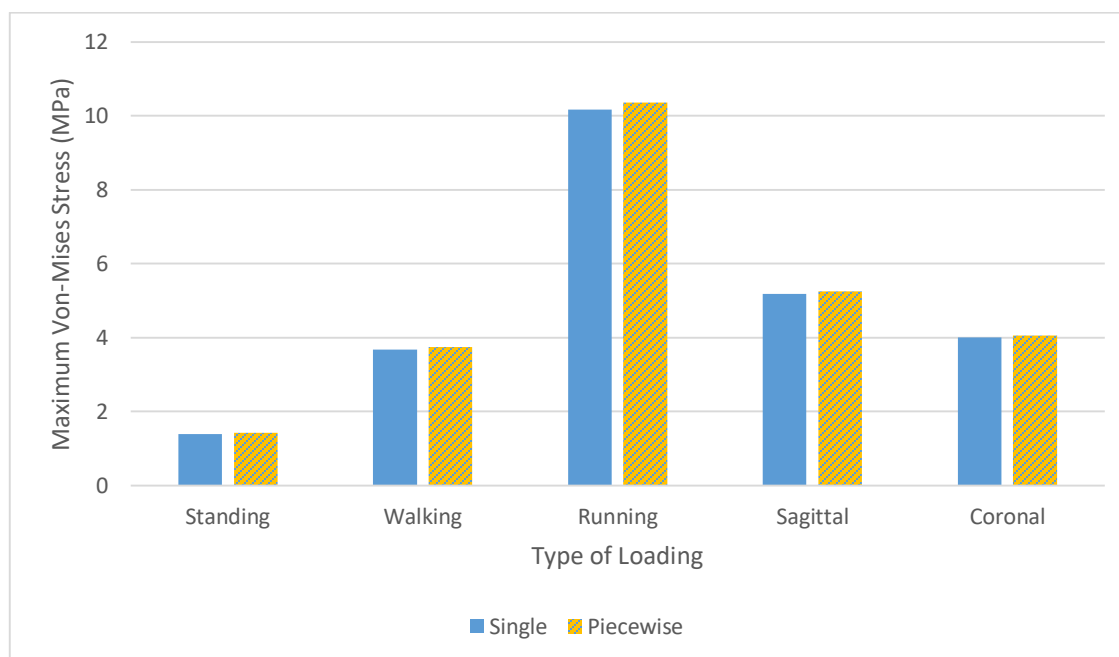


Fig. 5. Comparison of Von-Mises stress between single solid and cortical-cancellous (piecewise) model

For FE analysis with force applied on sagittal plane, the von-Mises stress were 5.18 MPa for single solid and 5.25 MPa and cortical-cancellous model, the percentage difference between the von-Mises stress of the two models is 1.324%. For coronal plane, the von-Mises stress observed for single solid and cortical-cancellous model were 4.00 MPa and 4.05 MPa respectively, with a percentage difference of 1.408%.

From the comparison of von-Mises stress between the single solid and cortical-cancellous 3D tibia models, it was observed that the percentage difference between the values of mechanical response fall under 2%, which means that the accuracy of results predicted with a simplified single body 3D model in FE analysis is comparable to the FE

analysis results with a more detailed model with both the cancellous bone and cortical bone modeled. It was also observed that all five sets of the simulations had the single 3D model yielded lower von-Mises stress compared to the cortical-cancellous model, this indicates that the results produced are consistent, which the single model yielding stress-strain response that corresponds to the cortical-cancellous model. Besides, the stress-strain distribution yielded of single model and cortical-cancellous model are also similar. In Figure 6, it is observed that the stress distribution in both of the models are similar with similar stress value, therefore there are very little difference between the FE analysis between single model and piecewise model.

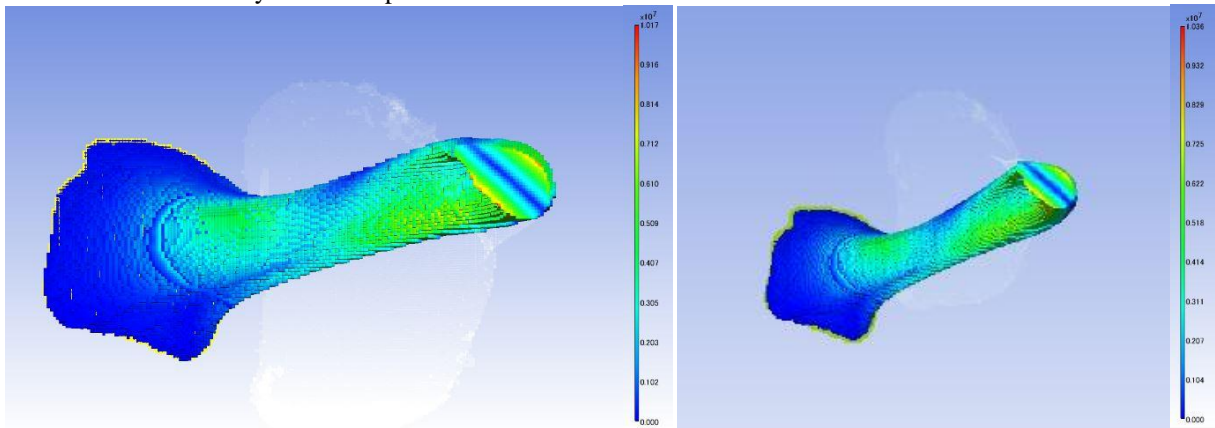


Fig. 6. Comparison of contour between single model (left) and piecewise model (right)

These findings are in accordant to previous researchers who studied on similar topic in determining the significance of the difference of FE results between single density and piecewise bone models. Fung et. al [19] concluded that cortical and cancellous bone of human metatarsals which are modelled separately independently didn't yield better FE simulation results compared to single density model. There are also studies conducted onto long bones as performed by Austman et. al and Cong et. al [20], [21] on ulna and femur respectively have found that single density modulus equation provides good FE simulation results as well, which is in line with the results in this study, and it was expected as tibia is also a long bone.

5. CONCLUSION

From the comparison of the FE analysis between a single solid OI tibia model and an OI tibia model with both cancellous and cortical bone of OI tibia bone, it is found that a single solid model yields a relatively accurate result compared to 3D model with cancellous and cortical components. The FE simulations were done with loads applied from different directions, therefore it can be concluded that a single model can yield accurate FE analysis results with cortical-cancellous model with respect to various types of loadings. Hence, for FE simulations involving OI tibia bone, the FE model can be simplified

into a single solid model which is less complicated than model with both cancellous and cortical bone configuration, this would help to save computing time and cost while still yielding satisfactory results.

ACKNOWLEDGEMENT

The authors would like to acknowledge the support from the Ministry of Education Malaysia under Fundamental Research Grant Scheme (FRGS) with grant number of FRGS/1/2016/TK03/UNIMAP/02/6.

REFERENCES

- [1] D. D. M. Sillence D O, Senn A, "Genetic heterogeneity in osteogenesis imperfecta," *J Med Genet*, vol. 16, p. 101, 1979.
- [2] A. Alhousseini et al., "A Non-Lethal Osteogenesis Imperfecta Type II Mutation.," *Gynecol. Obstet. Invest.*, vol. 48201, pp. 1–5, 2018.
- [3] N. Garijo, N. Verdonchot, K. Engelborghs, J. M. García-Aznar, and M. A. Pérez, "Subject-specific musculoskeletal loading of the tibia: Computational load estimation," *J. Mech. Behav. Biomed. Mater.*, vol. 65, pp. 334–343, 2017.
- [4] J. C. Gibbs, L. M. Giangregorio, A. K. O. Wong, R. G. Josse, and A. M. Cheung, "Appendicular and whole body lean mass outcomes are associated with finite element analysis-derived bone strength at the distal radius and tibia in adults aged 40 years and older," *Bone*, vol. 103, no. 2016, pp. 47–54, 2017.
- [5] K. Basaruddin, N. Takano, Y. Yoshiwara, and T. Nakano, "Morphology analysis of vertebral trabecular bone under dynamic loading based on multi-scale theory," *Med. Biol. Eng. Comput.*, vol. 50, no. 10, pp. 1091–1103, 2012.

- [6] K. S. Basaruddin, N. S. Kamarrudin, and I. Ibrahim, "Stochastic multi-scale analysis of homogenised properties considering uncertainties in cellular solid microstructures using a first-order perturbation," *Lat. Am. J. Solids Struct.*, vol. 11, pp. 755–769, 2014.
- [7] R. A. González-Carbonell, A. Ortiz-Prado, V. H. Jacobo-Armendáriz, Y. A. Cisneros-Hidalgo, and A. Alpízar-Aguirre, "3D patient-specific model of the tibia from CT for orthopedic use," *J. Orthop.*, vol. 12, no. 1, pp. 11–16, 2015.
- [8] Y. G. Koh, J. Son, S. K. Kwon, H. J. Kim, and K. T. Kang, "Biomechanical evaluation of opening-wedge high tibial osteotomy with composite materials using finite-element analysis," *Knee*, vol. 25, no. 6, pp. 977–987, 2018.
- [9] Y. Chevalier, D. Pahr, H. Allmer, M. Charlebois, and P. Zysset, "Validation of a voxel-based FE method for prediction of the uniaxial apparent modulus of human trabecular bone using macroscopic mechanical tests and nanoindentation," *J. Biomech.*, vol. 40, no. 15, pp. 3333–3340, Jan. 2007.
- [10] E. Schileo, F. Taddei, L. Cristofolini, and M. Viceconti, "Subject-specific finite element models implementing a maximum principal strain criterion are able to estimate failure risk and fracture location on human femurs tested in vitro," *J. Biomech.*, vol. 41, no. 2, pp. 356–367, 2008.
- [11] S. B. C. Wanna *et al.*, "Prediction on fracture risk of femur with Osteogenesis Imperfecta using finite element models: Preliminary study Prediction on fracture risk of femur with Osteogenesis Imperfecta using finite element models: Preliminary study," in *Journal of Physics: Conf. Series*, 2017, vol. 908, p. 012022.
- [12] S. B. C. Wanna *et al.*, "Fracture risk prediction on children with Osteogenesis Imperfecta subjected to loads under activity of daily living," in *IOP Conference Series: Materials Science and Engineering*, 2018, vol. 429, p. 012004.
- [13] R. Hambli and S. Allaoui, "A robust 3D finite element simulation of human proximal femur progressive fracture under stance load with experimental validation," *Ann. Biomed. Eng.*, vol. 41, no. 12, pp. 2515–2527, 2013.
- [14] P. W. Weng *et al.*, "The effects of tibia profile, distraction angle, and knee load on wedge instability and hinge fracture: A finite element study," *Med. Eng. Phys.*, vol. 42, pp. 48–54, 2017.
- [15] C. S. Rajapakse, E. A. Kobe, A. S. Batzdorf, M. W. Hast, and F. W. Wehrli, "Accuracy of MRI-based finite element assessment of distal tibia compared to mechanical testing," *Bone*, vol. 108, pp. 71–78, 2018.
- [16] C. Caouette *et al.*, "Biomechanical analysis of fracture risk associated with tibia deformity in children with osteogenesis imperfecta: a finite element analysis," *J. Musculoskelet. Neuronal Interact.*, vol. 14, no. 2, pp. 205–12, 2014.
- [17] I. Kutzner, B. Heinlein, F. Graichen, A. Bender, A. Rohlmann, and A. Halder, "Loading of the knee joint during activities of daily living measured in vivo in five subjects," *J. Biomech.*, vol. 43, no. 11, pp. 2164–2173, 2010.
- [18] D. J. Saxby *et al.*, "Gait & Posture Tibiofemoral contact forces during walking, running and sidestepping," *Gait Posture*, vol. 49, pp. 78–85, 2016.
- [19] A. Fung, L. L. Loundagin, and W. B. Edwards, "Experimental validation of finite element predicted bone strain in the human metatarsal," *J. Biomech.*, vol. 60, pp. 22–29, 2017.
- [20] R. L. Austman, J. S. Milner, D. W. Holdsworth, and C. E. Dunning, "The effect of the density-modulus relationship selected to apply material properties in a finite element model of long bone," *J. Biomech.*, vol. 41, no. 15, pp. 3171–3176, 2008.
- [21] A. Cong, J. O. Den Buijs, and D. Dragomir-Daescu, "In situ parameter identification of optimal density-elastic modulus relationships in subject-specific finite element models of the proximal femur," *Med. Eng. Phys.*, vol. 33, no. 2, pp. 164–173, 2011.